The Astrophysical Journal, 704:L108–L112, 2009 October 20 doi:10.1088/0004-637X/704/2/L108

MOLECULAR SURVIVAL IN EVOLVED PLANETARY NEBULAE: DETECTION OF H_2CO, c-C_3H_2, AND C_2H IN THE HELIX

E. D. Tenenbaum[1,2], S. N. Milam[3], N. J. Woolf[1], and L. M. Ziurys[1,2,4]
[1] Department of Astronomy & Steward Observatory, University of Arizona, 933 N. Cherry Avenue, Tucson, AZ 85721, USA; emilyt@as.arizona.edu, nwoolf@as.arizona.edu, lziurys@as.arizona.edu
[2] Department of Chemistry and Biochemistry, University of Arizona, 933 N. Cherry Avenue, Tucson, AZ 85721, USA
[3] SETI Institute, NASA Ames Research Center, M/S 245-6, Moffet Field, CA 94035, USA; Stefanie.N.Milam@nasa.gov
[4] Arizona Radio Observatory, University of Arizona, 933 N. Cherry Avenue, Tucson, AZ 85721, USA
Received 2009 July 20; accepted 2009 September 15; published 2009 October 5

ABSTRACT

H_2CO, c-C_3H_2, and C_2H have been identified in the neutral envelope of the highly evolved planetary nebula (PN), the Helix (also know as NGC 7293). Emission from these species were detected toward a peak position in CO, 372″ east of the central star, using the facilities of the Arizona Radio Observatory (ARO). C_2H and c-C_3H_2 were identified on the basis of their 3 mm transitions, measured with the ARO 12 m, while five lines of H_2CO were observed using the 12 m at 2 and 3 mm and the ARO Submillimeter Telescope at 1 mm. From a radiative transfer analysis of the formaldehyde emission, the molecular material was determined to have a density of $n(H_2)$ $\sim 3 \times 10^5$ cm^{-3}, with a kinetic temperature of T_{kin} ~20 K. Column densities for C_2H, H_2CO, and c-C_3H_2 of N_{tot} $\sim 1.4 \times 10^{13}$ cm^{-2}, 1.1×10^{12} cm^{-2}, and 3×10^{11} cm^{-2}, respectively, were derived, corresponding to fractional abundances relative to H_2 of $f(H_2CO) = 1 \times 10^{-7}$, f(c-C_3H_2) $= 3 \times 10^{-8}$, and $f(C_2H) = 1 \times 10^{-6}$. The physical conditions found support the notion that molecules in evolved PNe survive in dense clumps in pressure equilibrium, shielded from photodissociation. The presence of H_2CO, c-C_3H_2, and C_2H, along with the previously observed species CN, HNC, HCN, and HCO^+, indicates that a relatively complex chemistry can occur in the late stages of PN evolution, despite potentially destructive ultraviolet radiation. These molecules have also been observed in diffuse clouds, suggesting a possible connection between molecular material in evolved PNe and the diffuse ISM.

Key words: astrochemistry – ISM: molecules – planetary nebulae: individual (NGC 7293) – radio lines: ISM

1. INTRODUCTION

Intermediate-mass stars end their life cycle as planetary nebulae (PNe), a short-lived stage ($\sim 10^4$ yr) marked by a hot UV-emitting central white dwarf surrounded by an expanding envelope of ionized and neutral gas (Kwok 2000). Given the high UV flux, these objects should be an unsuitable environment for complex chemistry. Yet, in young PNe (post-asymptotic giant branch (AGB) age $\sim 10^3$ yr) a variety of molecules have been identified, including HCO^+, HCS^+, N_2H^+, CO^+, H_2O, SiS, CS, CN, HCN, HNC, C_2H, HC_3N, and c-C_3H_2 (Zhang et al. 2008 and references therein). The majority of these detections have occurred toward the well-studied source NGC 7027, but HCO^+, HCN, and CN have also been found in other young nebulae (Josselin and Bachiller 2003).

In contrast, the chemical content of evolved PNe (post-AGB age $\sim 10^4$ yr) has not been as extensively probed. Maps of $J = 2 \rightarrow 1$ emission of CO by Young et al. (1999) have shown that molecular gas is widespread across the Helix Nebula. The Helix is perhaps one of the oldest PNe known (age ~11,000 yr, Meaburn et al. 2008). Targeted studies of post-AGB objects by Bachiller et al. (1997) and Josselin & Bachiller (2003) have demonstrated the presence of CN, HCN, HNC, and HCO^+ toward several evolved PNe, including the Helix. Other species such as SiC_2 and HC_3N were not detected in these objects.

Theoretical chemical models predict that certain molecules can survive into the final stages of PNe, provided that the material is highly clumped. Howe et al. (1994) have predicted that both CN and C_2H would be present in the Helix in detectable quantities, protected in dusty knots. More recent chemical models by Ali et al. (2001) and Redman et al. (2003) also employ a clumpy medium. Ali et al. have in fact calculated abundances in evolved nebulae for HCN, HNC, CN, and HCO^+ that are in relatively good agreement with the observations; they also speculate that CH, CH_2, C_2H, HCl, OH, and H_2O are likely to be present in such objects. In contrast, Redman et al. severely underestimate molecular abundances in nebulae over 10,000 years old, although their calculations agree well with observations of younger objects. These authors suggest that molecular shielding is actually more effective than portrayed by their clumpy wind model.

Of all evolved PNe, the Helix, at a distance of 219 pc (Harris et al. 2007), is perhaps the best candidate for in-depth chemical studies. Previous measurements of He(III) emission have demonstrated that the innermost region of the nebula consists of highly ionized gas extending to a radius of ~100″. Beyond the He(III) core are two ellipsoidal rings with radii of ~240″ and ~370″, tilted 30° with respect to each other, and marked by emission in N(II) and S(II) (O'Dell et al. 2004). Molecular material, visible in 2.12 μm H_2 emission, first appears at the outer edge of the He(III) region in the form of small (~1″ diameter) dense, neutral knots (Speck et al. 2002). These knots extend well into the inner and outer rings (Speck et al. 2002; O'Dell et al. 2004), numbering between 20,000 and 40,000 (Hora et al. 2006). CO emission is also present, as mentioned, and extends over both ring regions to a radius of ~500″ (Young et al. 1999).

To further explore the chemical complexity in evolved PNe, we have conducted searches for other molecules in the Helix. We have detected C_2H, c-C_3H_2, and H_2CO at the position where CN, HCN, and HNC have been identified. Multiple formaldehyde lines have been observed, enabling an accurate determination of the gas density and temperature in this molecular material. Here we present our measurements and resulting molecular

abundances, and discuss their implications for chemistry in the late stages of stellar evolution.

2. OBSERVATIONS

All measurements were carried out between 2005 October and 2008 January using the telescopes of the Arizona Radio Observatory (ARO). The 2 and 3 mm observations were conducted with the ARO 12 m telescope on Kitt Peak, AZ. The receivers employed were dual polarization SIS mixers, operated in single-sideband mode with image rejection $\geqslant$17 dB. The backends used were two sets of 512 channel filter banks with 1 MHz and 0.5 MHz resolutions, respectively, split to accommodate the two receiver polarizations (i.e., parallel mode: 2 × 256 channels). The temperature scale, determined by the chopper-wheel method, is given in units of $T_R{}^*$ where $T_R = T_R{}^*/\eta_c$, and η_c is the corrected beam efficiency.

The 1 mm measurements were carried out with the ARO 10 m Submillimeter Telescope (SMT) on Mt. Graham, AZ. The receiver employed ALMA Band 6-type sideband-separating SIS mixers with a typical image rejection of ∼20 dB, accomplished in the mixer architecture. The backend used was a 1 MHz resolution filter bank configured in parallel mode (2 × 1024 channels). The temperature scale is determined by the chopper-wheel method, and is given as T_A^*, where $T_R = T_A^*/\ \eta_b$, and η_b is the beam efficiency.

Observations were done toward a single position in the eastern part of the nebula, offset by −372″ in R.A. from the central star (central star position: $\alpha = 22^{\rm h}26^{\rm m}54\overset{\rm s}{.}8$, $\delta = -21°05'41\overset{''}{.}0$, B1950.0). Data were taken in position-switching mode with a reference offset of 30′ in azimuth. Local oscillator shifts were done to test for image contamination and pointing and focus corrections were checked every ∼1.5 hr on planets. Observing frequencies, beam efficiencies, and beam sizes are given in Table 1.

3. RESULTS

Five transitions of H_2CO were detected toward the Helix: the fundamental line $J_{\rm Ka,Kc} = 1_{0,1} \rightarrow 0_{0,0}$ at 3 mm, the three asymmetry components of the $J = 2 \rightarrow 1$ transition at 2 mm ($J_{\rm Ka,Kc} = 2_{0,2} \rightarrow 1_{0,1}$, $2_{1,2} \rightarrow 1_{1,1}$, $2_{1,1} \rightarrow 1_{1,0}$), and one line at 1 mm ($J_{\rm Ka,Kc} = 3_{0,3} \rightarrow 2_{0,2}$). The transitions with $K_a = 0$ arise from the para stack, while those with $K_a = 1$ are ortho lines. Spectra are displayed in Figure 1.

Figure 2 shows two emission features of cyclic-C_3H_2: the $J_{\rm Ka,Kc} = 2_{0,2} \rightarrow 1_{1,1}$ transition of the para spin isomer, and the $J_{\rm Ka,Kc} = 2_{1,2} \rightarrow 1_{0,1}$ transition of the ortho isomer. Both c-C_3H_2 transitions have intensities of $T_R = 7$–8 mK. An attempt to observe the $J_{\rm Ka,Kc} = 2_{2,1} \rightarrow 1_{1,0}$ line at 122 GHz was unsuccessful due to high atmospheric water vapor (3σ upper limit: 23 mK).

The two hyperfine lines of the $J = 3/2 \rightarrow 1/2$ fine structure component of the $N = 1 \rightarrow 0$ rotational transition of C_2H were observed, displayed in Figure 3. As shown, the $F = 2 \rightarrow 1$ and $1 \rightarrow 0$ components are fully resolved because the hyperfine splitting (40 km s^{-1}) is larger than the linewidth (∼7 km s^{-1}). The observed intensity ratio of the C_2H lines is consistent with the intrinsic line strengths, as indicated underneath the spectrum (Ziurys et al. 1982).

Table 1 lists the line parameters of the observed features. All transitions appear as single features at LSR velocities of ∼ −15 km s^{-1}, with linewidths ranging from 4 to 7 km s^{-1}, consistent with other molecular lines observed toward this position (Bachiller et al. 1997). The +9 km s^{-1} shift of the emission with respect to the central star velocity of −24 km s^{-1} is due to the complex expansion structure of the Helix nebula.

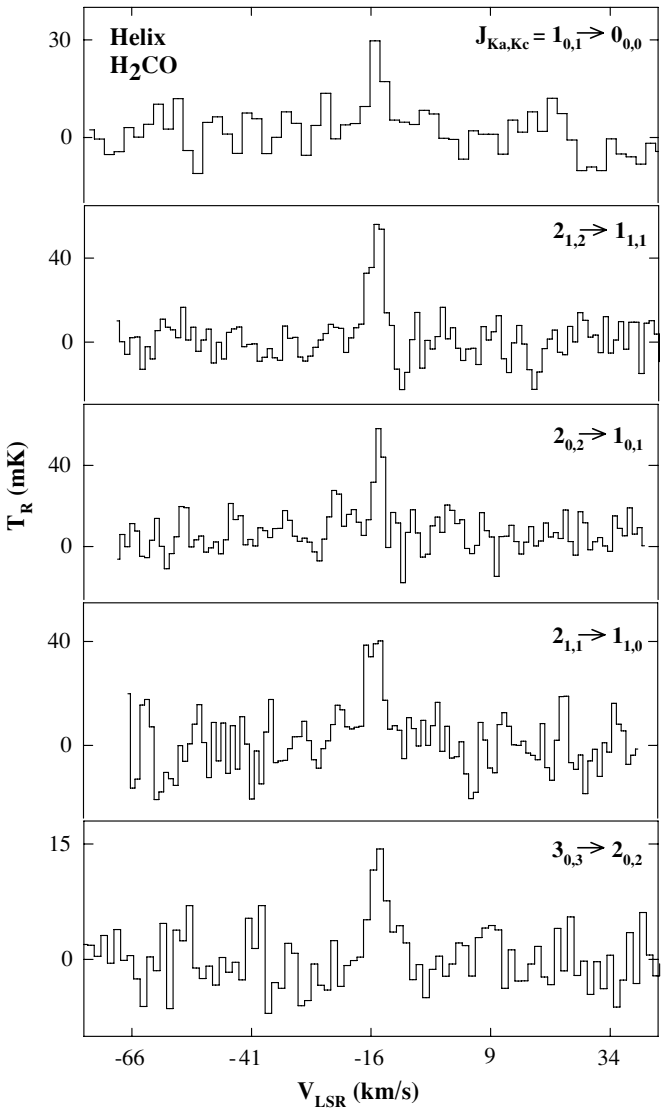

Figure 1. Spectra of the five H_2CO transitions detected in the range 72–218 GHz toward the neutral envelope of the Helix Nebula. The $J_{\rm Ka,Kc} = 1_{0,1} \rightarrow 0_{0,0}$ (73 GHz), $2_{1,2} \rightarrow 1_{1,1}$ (141 GHz), $2_{0,2} \rightarrow 1_{0,1}$ (146 GHz), and $2_{1,1} \rightarrow 1_{1,0}$ (150 GHz) lines of this molecule were observed with the ARO 12 m, while the $3_{0,3} \rightarrow 2_{0,2}$ transition (218 GHz) was measured with the ARO SMT. Spectral resolution is 500 kHz for all transitions except the one at 218 GHz, which was measured with 1 MHz resolution. Integration times fall in the range ∼6–40 hr.

4. ANALYSIS

The critical densities of the upper levels of the observed formaldehyde transitions range from 1 × 10^5 to 3 × 10^6 cm^{-3}, and the energies span 3–23 K, making this molecule ideal for constraining physical conditions. To model the H_2CO lines, the RADEX non-LTE radiative transfer program was used (van der Tak et al. 2007)[5]. This code solves the statistical equilibrium equations for collisional and radiative processes for a given gas kinetic temperature, density, and molecular column density, and then predicts line intensities. In the one-dimensional RADEX program, the escape probability formulation is utilized assuming

[5] http://www.strw.leidenuniv.nl/∼moldata/radex.html

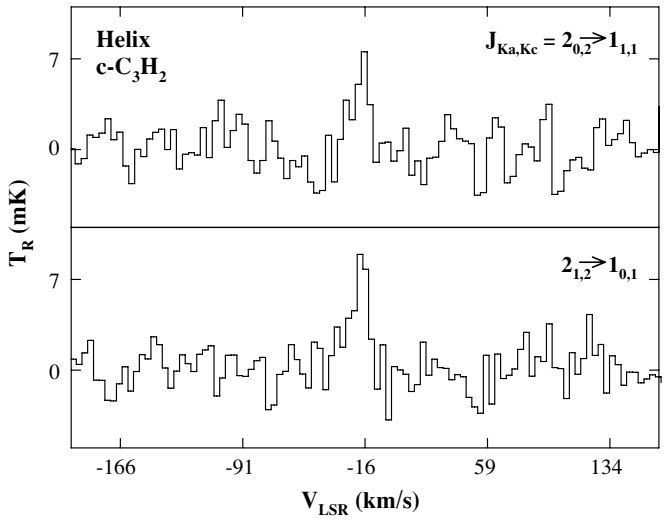

Figure 2. Spectra of the two transitions of c-C_3H_2 observed toward the Helix with the ARO 12 m telescope at 3 mm: the ortho $J_{Ka,Kc} = 2_{1,2} \rightarrow 1_{0,1}$ line at 85 GHz and the para $2_{0,2} \rightarrow 1_{1,1}$ line at 82 GHz. Spectral resolution is 1 MHz. Integration times are 13 and 18 hr, respectively.

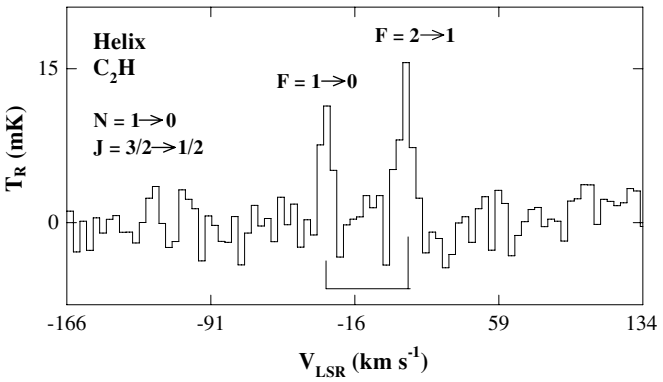

Figure 3. Spectra of the $F = 2 \rightarrow 1$ and $1 \rightarrow 0$ hyperfine components of the $J = 3/2 \rightarrow 1/2$ spin-rotation doublet of the $N = 1 \rightarrow 0$ transition of the C_2H radical, observed toward the Helix with the ARO 12 m telescope at 87 GHz. The spectral resolution is 1 MHz. The frequencies and relative intensities of the hyperfine components are indicated underneath the spectrum. These data were acquired in 14 hr.

an isothermal, homogeneous medium, with geometry and large-scale motion left unspecified. We used ortho-H_2CO with para-H_2 collisional rates from Troscompt et al. (2009), and para-H_2CO with para-H_2 rates provided by A. Faure & N. Troscompt (2009, private communication).

For this analysis, calculations were carried out over a grid of conditions covering five temperatures from 10 to 50 K, nineteen H_2 gas densities spanning 5×10^4 to 5×10^6 cm^{-3}, and sixteen H_2CO column densities ranging from 8×10^{11} to 5×10^{13} cm^{-2}. Two source distributions were considered: one where the emission fills the telescope beams (beam filling factor = 1), and another with $\theta_s = 25''$. A chi-squared analysis was done to determine the physical parameters that best reproduced the observed emission. In the case where the source fills the telescope beams, excellent agreement was found between predicted and observed values for $T_{kin} = 20$ K, $n(H_2) = 3 \times 10^5$ cm^{-3}, and $N_{tot}(H_2CO) = 1 \times 10^{12}$ cm^{-2} (assuming ortho:para = 3:1). In the simulations with $\theta_s = 25''$, similarly good agreement was not achieved, and the best chi-squared value in this case was over 30 times larger than for the extended source analysis. As an additional check, the rotational diagram method was used, resulting in $N_{tot}(H_2CO) \simeq 1.1 \times 10^{12}$ cm^{-2} and $T_{rot} \simeq 8$ K. This column density is in good agreement with the radiative transfer results, and the rotational temperature indicates subthermal excitation, which would be expected for H_2CO in this gas, with $\mu_a = 2.3$ D (Fabricant et al. 1977).

Modeling of the c-C_3H_2 lines was then carried out with RADEX assuming an extended source and the physical conditions based on the H_2CO results. The best agreement between observations and model predictions was attained for N_{tot}(c-C_3H_2) $= 3 \times 10^{11}$ cm^{-2}, again using ortho:para = 3:1. Collisional excitation rates were from Chandra & Kegel (2000).

For C_2H, collisional excitation rates are not known. Therefore, the column density was calculated assuming optically thin, extended emission, and a rotational temperature of 20 K, resulting in $N_{tot} = 1.4 \times 10^{13}$ cm^{-2}. The low dipole moment of C_2H (0.77 D; Woon 1995) will ensure thermal excitation, thus justifying the assumption $T_{rot} = T_{kin}$.

To determine fractional abundances, relative to H_2, it was assumed that the ratio of the column densities between a given molecule and CO is equivalent to the ratio of fractional abundances:

$$\frac{N_{tot}(X)}{N_{tot}(CO)} = \frac{f(X/H_2)}{f(CO/H_2)}. \quad (1)$$

Table 1
Molecular Observations Toward the Helix Nebula (NGC 7293)

Molecule	Transition	ν (MHz)	θ_b ($''$)	η_c	T_R (mK)	$\Delta V_{1/2}$ (km s^{-1})	V_{LSR} (km s^{-1})	$\int T_R\, dv$ (K km s^{-1})
C_2H	$N = 1 \rightarrow 0$							
	$J = 3/2 \rightarrow 1/2$							
	$F = 2 \rightarrow 1$	87316.9	72	0.91	14 ± 2	6.9 ± 3.4	−15.1 ± 3.4	0.12 ± 0.05
	$F = 1 \rightarrow 0$	87328.6	72	0.91	10 ± 2	6.9 ± 3.4	−16.4 ± 3.4	0.10 ± 0.05
H_2CO	$J_{Ka,Kc} = 1_{0,1} \rightarrow 0_{0,0}$	72837.9	86	0.94	26 ± 5	4.1 ± 2.1	−14.1 ± 2.1	0.18 ± 0.06
	$J_{Ka,Kc} = 2_{1,2} \rightarrow 1_{1,1}$	140839.5	45	0.76	53 ± 5	4.2 ± 1.1	−15.6 ± 1.1	0.21 ± 0.05
	$J_{Ka,Kc} = 2_{0,2} \rightarrow 1_{0,1}$	145602.9	43	0.75	47 ± 7	3.1 ± 1.0	−15.0 ± 1.0	0.13 ± 0.05
	$J_{Ka,Kc} = 2_{1,1} \rightarrow 1_{1,0}$	150498.3	42	0.74	36 ± 10	4.0 ± 1.0	−14.4 ± 1.0	0.15 ± 0.04
	$J_{Ka,Kc} = 3_{0,3} \rightarrow 2_{0,2}$	218222.2	35	0.77[a]	13 ± 3	4.1 ± 1.4	−14.3 ± 1.4	0.06 ± 0.03
c-C_3H_2	$J_{Ka,Kc} = 2_{0,2} \rightarrow 1_{1,1}$	82093.6	77	0.92	7 ± 2	7.4 ± 3.6	−15.6 ± 3.6	0.10 ± 0.05
	$J_{Ka,Kc} = 2_{1,2} \rightarrow 1_{0,1}$	85338.9	74	0.91	8 ± 2	7.0 ± 3.5	−19.1 ± 3.5	0.11 ± 0.05
	$J_{Ka,Kc} = 2_{2,1} \rightarrow 1_{1,0}$	122023.5	52	0.81	$\leqslant 23$			$\leqslant 0.16$

Note.
[a] η_b.

Table 2
Molecular Abundances in the Helix Versus Diffuse Clouds

Molecule	Helix	Diffuse Cloud[a]
H_2CO	1×10^{-7}	4×10^{-9}
c-C_3H_2	3×10^{-8}	1×10^{-9}
C_2H	1×10^{-6}	3×10^{-8}
CO	9×10^{-4}	3×10^{-6}
CN	3×10^{-6} [b]	2×10^{-8}
HCN	5×10^{-7} [b]	3×10^{-9}
HNC	3×10^{-7} [b]	6×10^{-10}
HCO^+	2×10^{-7} [b]	2×10^{-9}

Notes.
[a] From Liszt et al. (2006).
[b] Derived from Bachiller et al. (1997); see the text.

Here we adopted a CO column density of 8.9×10^{15} cm^{-2}, reported toward the same position in the Helix (Bachiller et al. 1997). The CO fractional abundance was estimated by assuming that all the oxygen is contained in CO (Young et al. 1997) and all hydrogen in H_2, and using an O/H ratio of 4.6×10^{-4}, determined from optical observations (Henry et al. 1999). These assumptions yield $f(CO/H_2) \sim 9 \times 10^{-4}$. Fractional abundances thus derived are $f(H_2CO/H_2) \sim 1 \times 10^{-7}$, f(c-C_3H_2/H_2) $\sim 3 \times 10^{-8}$, and $f(C_2H/H_2) \sim 1 \times 10^{-6}$. Using the same method, fractional abundances of HCN, HNC, HCO^+, and CN were additionally calculated from column densities of Bachiller et al. (1997). A summary of these values is presented in Table 2.

5. DISCUSSION

5.1. Chemical Abundances and Model Predictions

Toward the region of the Helix studied in this work, C_2H is the fourth most abundant molecule after H_2, CO, and CN. The fractional abundance of CO, $f \sim 9 \times 10^{-4}$, is typical of carbon-rich gas (see Ziurys et al. 2009), while those of CN and C_2H are near $f \sim 10^{-6}$ (see Table 2). The prominence of CN and C_2H is not surprising; the two radicals are photodissociation products and are predicted to be abundant in evolved PNe. For example, both Ali et al. (2001) and Howe et al. (1994) estimate a fractional abundance of C_2H near 10^{-6}, although Redman et al. (2003) predict $f(C_2H/H_2) \sim 7 \times 10^{-10}$, three orders of magnitude lower.

C_2H has also been detected in the proto-PNe CRL 618 (Pardo & Cernicharo 2007) and CRL 2688 (Fuente et al. 1998), as well as the young PN NGC 7027 (Zhang et al. 2008). In NGC 7027, the abundance of this radical is 5.4×10^{-8}. In C-rich AGB envelopes, the presence of C_2H varies widely, ranging from abundances as high as 1.5×10^{-5}, to lower limits of $<1.0 \times 10^{-7}$ (Woods et al. 2003).

Formaldehyde has an estimated abundance of $f \sim 1 \times 10^{-7}$. To our knowledge, this molecule has yet to be considered in chemical modeling of PNe. H_2CO also appears to be particularly prominent toward the C-rich PPN CRL 618 (Pardo et al. 2007). In addition, there is evidence for formaldehyde in the O-rich PPN OH 231.8+4.2 (Lindqvist et al. 1992) and the evolved PNe IC 4406 and NGC 6072 (Woods & Nyman 2005). Surprisingly, H_2CO has not yet been observed in young PNe; Zhang et al. (2008) reported only upper limits toward NGC 7027. This molecule appears to be less prevalent in AGB envelopes. It has only been detected in IRC +10216 with an abundance of 1.4×10^{-9} (Saavik Ford et al. 2004; Agúndez & Cernicharo 2006).

Compared to the other molecules listed in Table 2, a relatively low concentration of c-C_3H_2 ($f = 3 \times 10^{-8}$) exists in the Helix. Chemical modeling predictions in PNe are not available for this species; however, c-C_3H_2 has been observed with similar abundances in the young PN NGC 7027 ($f \sim 1 \times 10^{-8}$; Fuente et al. 2003) and in two carbon-rich AGB envelopes ($f \sim 3$–60×10^{-8}; Woods et al. 2003).

5.2. Physical Characteristics of the Gas

The position used for these observations is 1.2×10^{18} cm east of the central star, on the periphery of the ionized nebula. At this location, the H_2CO data indicate a gas density of 3×10^5 cm^{-3} and $T_{kin} \sim 20$ K. Note that in the interclump medium, the density and kinetic temperature are estimated to be 120 cm^{-3} and 10^4 K, respectively (Henry et al. 1999), consistent with the notion of pressure equilibrium. Bachiller et al. (1997) derived a density of 1–4×10^5 cm^{-3} toward the same position in the Helix, from the $N = 1 \rightarrow 0$ and $N = 2 \rightarrow 1$ lines of CN, assuming $T_{kin} \sim 25$, in good agreement. O'Dell et al. (2005) reported $n(H_2) = 1 \times 10^6$ cm^{-3} in the core of one cometary knot, established from analysis of H_2, CO, and dust extinction, and Hora et al. (2006) found $n(H_2) = 1 \times 10^5$ cm^{-3} from modeling H_2 lines observed with *Spitzer*. Maps of the $J = 1 \rightarrow 0$ transition of HCO^+ across the Helix suggest that these high densities exist throughout the nebula (L. N. Zack & L. M. Ziurys 2010, in preparation).

The molecular gas observed must consist of many clumps filling the line of sight. If this material were confined to a single, uniform sphere with a radius of 30″, the derived density implies a mass of 2 $M_\odot$. Such a value is highly unlikely considering the wide spatial extent of the molecular envelope and the estimated Helix progenitor mass of 6.5 $M_\odot$ (Henry et al. 1999). Moreover, mapping of the $J = 2 \rightarrow 1$ transition of CO indicates an aggregated medium with clump sizes on the order of ∼15″ (Young et al. 1999). The detection of C_2H and c-C_3H_2 in the Helix is further evidence that this nebula is carbon rich. There has been some uncertainty in the literature about the elemental C/O ratio in this source. Measurements by Henry et al. (1999) of atomic emission lines in the Helix suggested that O > C. However, the presence of CN, HCN, and HNC has been used as evidence for carbon enrichment (Cox et al. 1998). These three species, on the other hand, have recently been observed in O-rich circumstellar envelopes, and therefore do not necessarily indicate C > O (Ziurys et al. 2009). Stronger evidence for a C-rich composition is derived from the detection ofreseno.009 242.44527.

The origin of the molecules observed in the Helix is uncertain. They are perhaps being produced from species generated in the young PNe phase. Ion–molecule and radical–radical reactions, photochemistry, and shock chemistry could all potentially be playing a role. For example, the dissociative recombination of $C_3H_3^+$ could produce c-C_3H_2 (Nejad & Millar 1987)—highly plausible in the Helix, given the large extent and observed abundance of HCO^+ (Bachiller et al. 1997; L. N. Zack & L. M. Ziurys 2010, in preparation). Radical reactions could be significant, such as (Agúndez & Cernicharo 2006):

$$O + CH_3 \rightarrow H_2CO + H. \quad (2)$$

Photochemistry certainly occurs in the Helix envelope; CN and C_2H are likely photodissociation products of HCN and HCCH, respectively. Another less certain mechanism is the formation of c-C_3H_2 from photodissociation of large aromatic molecules (Fuente et al. 2003; Teyssier et al. 2004), but it is unclear whether such aromatics exist in the Helix (Hora et al. 2006). Shocks could also drive the chemistry, as suggested by rovibrational lines of H_2 (Hora et al. 2006).

Eventually the pressure equilibrium that allows dense clumps to exist in the Helix will cease and the neutral molecular envelope will dissipate into the diffuse interstellar medium, possibly seeding the diffuse gas with molecular material. Over the past decade, a number of polyatomic species have been detected in diffuse clouds via millimeter-wave absorption (see Liszt et al. 2006 and references therein). The diffuse cloud abundances of many of these molecules, including H_2CO, c-C_3H_2, and C_2H, cannot be accounted for by in situ gas-phase formation mechanisms (Snow & McCall 2006). One explanation is that PNe feed some fraction of molecular matter to diffuse clouds. Since the majority of the clouds studied by Liszt et al. lie at fairly high Galactic latitude, they are more likely linked to dying A, F, and G stars, which have a broad distribution in latitude, rather than GMCs, which hug the Galactic plane. At high galactic latitudes, the number density of PNe is ~ 4 kpc^{-3}, with the average distance between the nebulae being less than $\sim$500 pc (calculated from Acker et al. 1994). In $\sim 10^7$ yr, a clump with $n \sim 3 \times 10^5$ cm^{-3} will dissipate into diffuse material with $A_v = 1$ (Price et al. 2003; Redman et al. 2003), and thus travel $\sim$150 pc, assuming $V_{\rm exp} = 15$ km s^{-1}. It is therefore apparent that remnant PN material moves well away from its parent star and can enrich diffuse clouds.

A comparison of molecular abundances in the Helix with those found in diffuse clouds is given in Table 2 to examine the hypothesis that PNe feed molecular matter into the diffuse ISM. The abundances in the Helix are generally one order of magnitude larger than in diffuse clouds, a difference that could be attributed to the gradual photodestruction of molecules in the transition to diffuse clouds. Redman et al. (2003) point out that molecules with slow photodissociation rates, such as benzene, can survive in the ejecta from PNe and may establish abundances in the diffuse interstellar medium. Furthermore, clump dissipation is obviously slower than previously thought (see above and Redman et al. 2003). Molecules may also freeze out onto grain surfaces in the late PN stage, and then later return to the gas phase in diffuse clouds by photodesorption.

Additional observations toward the Helix, both at different positions and in other molecular species, are needed to further examine the extent of its chemistry. Sensitive studies are imperative toward other sources, as well. Such measurements will help establish the physical and chemical properties of PNe, and increase our understanding of the final stages of intermediate mass stars and their contribution to the overall cycling of material in the ISM.

We thank A. Faure and N. Troscompt for their unpublished para-H_2CO collisional rates. This research is funded by NSF grant AST-0607803. E.D.T. acknowledges support from the NSF Graduate Research Fellowship Program.

REFERENCES

Acker, A., et al. 1994, VizieR Online Data Catalog, 5084, 0
Agúndez, M., & Cernicharo, J. 2006, ApJ, 650, 374
Ali, A., Shalabiea, O. M., El-Nawawy, M. S., & Millar, T. J. 2001, MNRAS, 325, 881
Bachiller, R., Forveille, T., Huggins, P. J., & Cox, P. 1997, A&A, 324, 1123
Chandra, S., & Kegel, W. H. 2000, A&AS, 142, 113
Cox, P. 1998, ApJ, 495, L23
Fabricant, B., Krieger, D., & Muenter, J. S. 1977, J. Chem. Phys., 67, 1576
Fuente, A., Cernicharo, J., & Omont, A. 1998, A&A, 330, 232
Fuente, A., Rodríguez-Franco, A., García-Burillo, S., Martín-Pintado, J., & Black, J. H. 2003, A&A, 406, 899
Harris, H. C., et al. 2007, AJ, 133, 631
Henry, R. B. C., Kwitter, K. B., & Dufour, R. J. 1999, ApJ, 517, 782
Hora, J. L., Latter, W. B., Smith, H. A., & Marengo, M. 2006, ApJ, 652, 426
Howe, D. A., Hartquist, T. W., & Williams, D. A. 1994, MNRAS, 271, 811
Josselin, E., & Bachiller, R. 2003, A&A, 397, 659
Kwok, S. 2000, The Origin and Evolution of Planetary Nebulae (Cambridge, UK: Cambridge Univ. Press)
Lindqvist, M., Olofsson, H., Winnberg, A., & Nyman, L. 1992, A&A, 263, 183
Liszt, H. S., Lucas, R., & Pety, J. 2006, A&A, 448, 253
Meaburn, J., López, J. A., & Richer, M. G. 2008, MNRAS, 384, 497
Nejad, L. A. M., & Millar, T. J. 1987, A&A, 183, 279
O'Dell, C. R., Henney, W. J., & Ferland, G. J. 2005, AJ, 130, 172
O'Dell, C. R., McCullough, P. R., & Meixner, M. 2004, AJ, 128, 2339
Pardo, J. R., & Cernicharo, J. 2007, ApJ, 654, 978
Pardo, J. R., Cernicharo, J., Goicoechea, J. R., Guélin, M., & Asensio Ramos, A. 2007, ApJ, 661, 250
Price, R. J., Viti, S., & Williams, D. A. 2003, MNRAS, 343, 1257
Redman, M. P., Viti, S., Cau, P., & Williams, D. A. 2003, MNRAS, 345, 1291
Saavik Ford, K. E., Neufeld, D. A., Schilke, P., & Melnick, G. J. 2004, ApJ, 614, 990
Snow, T. P., & McCall, B. J. 2006, ARA&A, 44, 367
Speck, A. K., Meixner, M., Fong, D., McCullough, P. R., Moser, D. E., & Ueta, T. 2002, AJ, 123, 346
Teyssier, D., Fossé, D., Gerin, M., Pety, J., Abergel, A., & Roueff, E. 2004, A&A, 417, 135
Troscompt, N., Faure, A., Wiesenfeld, L., Ceccarelli, C., & Valiron, P. 2009, A&A, 493, 687
van der Tak, F. F. S., Black, J. H., Schöier, F. L., Jansen, D. J., & van Dishoeck, E. F. 2007, A&A, 468, 627
Woods, P. M., & Nyman, L.-Å. 2005, in IAU Symp. 231, Astrochemistry: Recent Successes and Current Challenges, ed. A. J. Markwick-Kemper (San Francisco, CA: ASP), 326
Woods, P. M., Schöier, F. L., Nyman, L.-Å., & Olofsson, H. 2003, A&A, 402, 617
Woon, D. E. 1995, Chem. Phys. Lett., 244, 45
Young, K., Cox, P., Huggins, P. J., Forveille, T., & Bachiller, R. 1997, ApJ, 482, L101
Young, K., Cox, P., Huggins, P. J., Forveille, T., & Bachiller, R. 1999, ApJ, 522, 387
Zhang, Y., Kwok, S., & Dinh-V-Trung, 2008, ApJ, 678, 328
Ziurys, L. M., Saykally, R. J., Plambeck, R. L., & Erickson, N. R. 1982, ApJ, 254, 94
Ziurys, L. M., Tenenbaum, E. D., Pulliam, R. L., Woolf, N. J., & Milam, S. N. 2009, ApJ, 695, 1604